Porous Silicon Formation by Photoetching

Sadao Adachi

Contents

Abstract

This updated literature review concerns the photoetching technique of preparing photoluminescent mesoporous silicon films using hydrofluoric acid-based electrolytes, alkaline electrolytes, and aqueous alkali salt solutions. The photoetching mechanisms and types of porous silicon layers created are discussed. The benefits of using an incoherent light source and specific oxidizing agents are highlighted. The technique is particularly useful for creating thin porous regions in *n*-type Si wafers, SOI wafers, micromachined wafers, or those that contain electronic circuitry. Photoetching has also recently been developed for nanostructuring inexpensive silicon powder feedstocks.

Keywords

Electron affinity · Photoetching · Photoluminescence · Porous silicon (PS) · Redox potential

---

S. Adachi (✉)
Division of Electronics and Informatics, Faculty of Science and Technology, Gunma University, Gunma, Kiryu-shi, Japan
e-mail: adachi@gunma-u.ac.jp

L. Canham (ed.), *Handbook of Porous Silicon*,
https://doi.org/10.1007/978-3-319-71381-6_6

Introduction

Visible photoluminescence (PL) from porous silicon (PS) observed at room temperature has inspired sustained research into its potential application in Si-based optoelectronic devices and its theoretical basis (Canham 1990). This property is reviewed in the handbook chapter “Photoluminescence of Porous Silicon.” Most PS layers are prepared by anodic etching on *p*-type Si substrates, a technique in which metal is often deposited on the rear surface of the Si substrate in order for it to be used as an ohmic back contact (see handbook chapter ▶ “Porous Silicon Formation by Anodization”). However, the requirement for a back contact electrode is a limitation of this method; for example, it is difficult to form a PS layer on a silicon-on-insulator (SOI) structure or on Si integrated circuits. A photoetching method, on the other hand, requires no electrodes and allows the formation of a visible luminescence layer on not only single-crystalline Si substrates but also SOI structures.

Photoetching Setup

An experimental setup used for the formation of PS by photoetching is shown in Fig. 1 (Xu and Adachi 2006). The sample surface is illuminated by a Xe lamp through an optical filter that blocks wavelengths shorter than 600 nm. The use of an optical filter is to block the heat rays from the Xe lamp. A laser, a W lamp, or another light source may be used instead of a Xe lamp. The use of an incoherent light source such as a Xe or W lamp enables the formation of a large and homogeneous PS layer. Typically, an *n*-type Si wafer is immersed in an etchant solution of HF. The addition of an oxidant (e.g., H_2O_2 or I_2) to the HF solution results in the stable formation of PS layers in a short time period.

n-Si/Electrolyte Interface and Photoetching Reaction

Figure 2 shows the energy band diagrams for *n*-Si electrodes in pure HF (pH = 2.3) and HF/oxidant solutions without and with light illumination (Xu and Adachi 2006). The electron affinity (χ_s) of Si is −4.05 eV. At zero pH, the redox coupling is defined as the normal hydrogen electrode with a potential of −4.5 eV with respect to vacuum. This potential shifts toward more positive values with the increase in pH (+0.059 eV/pH). Thus, the electron energy of the pure HF solution with respect to vacuum is −4.36 eV (χ_l). The Fermi levels (E_{F} and $E_{\mathrm{F,redox}}$) on both sides of the *n*-Si/electrolyte interface are brought to the same energy level by a transfer of electrons from the Si substrate to the electrolyte (Fig. 2a).

The half reaction for the oxidizing agent KIO_3 is

$$\mathrm{IO_3^-} + 6\mathrm{H}^+ + 6\mathrm{e}^- = \mathrm{I}^- + 3\mathrm{H_2O} \quad (E^{\mathrm{o}} = 1.085\ \mathrm{eV})$$

where e^- represents the electron and E^{o} is the standard reduction potential with respect to the standard hydrogen electrode. The redox potential (E_{abs}) with respect to

Fig. 1 Experimental setup used for porous silicon formation by photoetching in an HF/oxidant solution

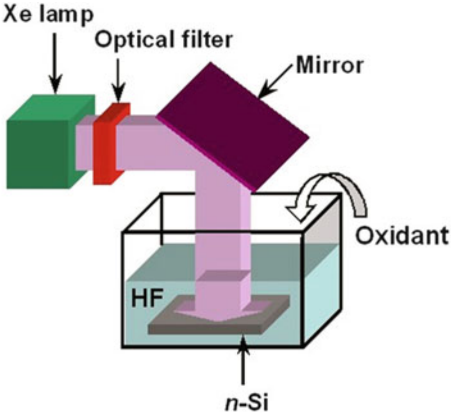

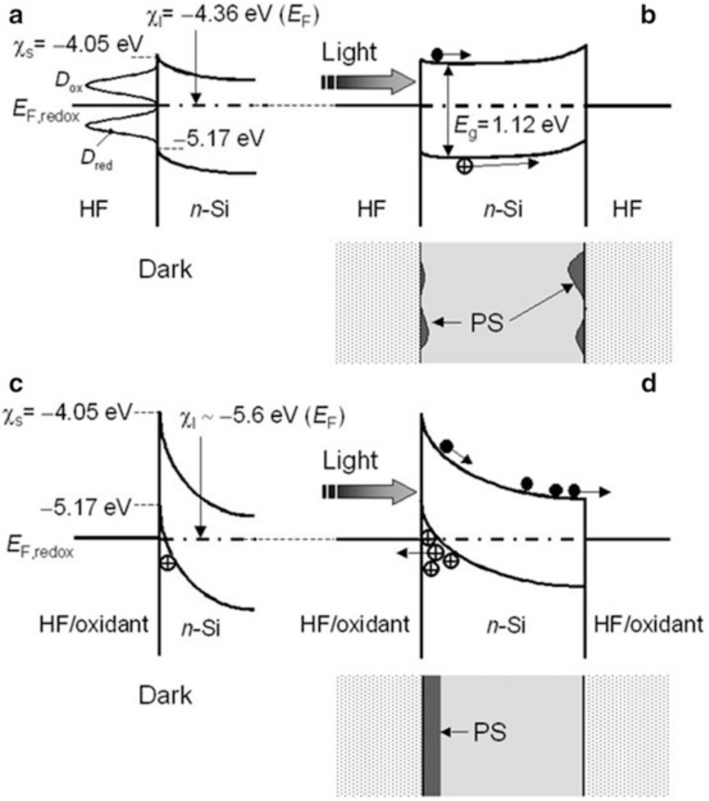

Fig. 2 Energy band diagram for *n*-Si immersed in pure HF solution (**a**, **b**) and those in HF/KIO_3 solution (**c**, **d**). In (**b**), porous silicon (PS) is formed stably on the back side in opposition to the illuminated surface. In (**d**), PS is formed only on the illuminated surface

vacuum for the HF/KIO_3 redox system is then given by $E_{abs} = -4.5 - E^o = -5.6$ eV (Fig. 2c). It is to be noted that the larger the E^o value is in the positive (negative) scale, the stronger is the oxidation (reduction) agent (Adachi and Kubota 2007; Xu and Adachi 2007; Tomioka et al. 2007).

The absorption of photons results in the generation of electron-hole pairs. The holes at the *n*-Si/electrolyte interface can participate in PS formation. In the case of the pure HF solution (Fig. 2b), the photoexcited holes are hard to drift toward the surface by the very small downward band bending or possibly by the almost-flat band. Thus, efficient PS formation cannot be expected in pure HF solution. When the Si wafer is dipped in the HF/oxidant solution (Fig. 2d), on the other hand, many photoexcited holes move toward the *n*-Si/electrolyte interface at the front surface, resulting in the formation of PS with good reproducibility (Xu and Adachi 2006, 2007; Adachi and Kubota 2007; Tomioka et al. 2007).

Reproducibility has been observed to be problematic in the formation of PS by photoetching, as with stain etching (see handbook chapter "▶ Porous Silicon Formation by Stain Etching"). In an extreme case, no PS layer was formed on the front surface, although surprisingly PS was formed on the surface of the sample that was not exposed to illumination (i.e., on the back surface) (Andersen et al. 1995). The effectiveness of surface cleaning by sulfuric peroxide mixture (SPM) treatment or by KOH etching before PS formation has been reported in Tomioka et al. (2007) and Andersen et al. (1995).

The photo-illuminated *n*-Si/aqueous NH_4F interface has been shown to form a hydrogenated amorphous Si overlayer which builds up progressively as photoetching proceeds with disproportionation of Si^{2+} species in solution (Peter et al. 1989). It is known that a galvanic cell is formed when a *p*-type Si is contacted with a noble metal in a HF/oxidant solution (Kobayashi and Adachi 2010). This galvanic cell leads to metal-assisted etching of *p*-Si, resulting in the formation of Si nanowire arrays. PS layers prepared by two routes, metal-assisted etching and laser-induced etching, have been studied by comparing surface morphologies using scanning electron microscopy (Kobayashi and Adachi 2010; Saxena et al. 2015). A PL peak at ~1.8 – 2.0 eV corresponding to red emission at room temperature was observed from such *p*-Si samples. The fact suggests that the PS layers can be formed not only on the laser-etched surfaces but also on the Si nanowire arrays formed by metal-assisted electroless etching. In *p*-Si prepared by laser etching, wider pores with some variation in pore size as compared to metal-assisted etching technique were observed because a HeNe laser having Gaussian profile of intensity was used for porosification (Saxena et al. 2015).

PS Layers Formed by Photoetching

A summary of PS formation by photoetching is presented in Tables 1 and 2 (Noguchi and Suemune 1993; Zhang et al. 1993; Cheah and Choy 1994; Andersen et al. 1995; Jones et al. 1996; Kolasinski et al. 2000; Yamamoto and Takai 2000, 2001; Mavi et al. 2001, 2006; Koker et al. 2002; Marotti et al. 2003; Zheng et al. 2005; Tomioka and Adachi 2005; Adachi and Tomioka 2005; Cho et al. 2006; Xu and

Table 1 Photoetching for porous silicon formation in acidic solutions

Type (Ω cm)	Solution	Light source	PL peak energy (eV)	Comments	References
n (0.01–15)	50% HF	HeNe laser, Xe lamp	~1.8	No PS formation when excited at $\lambda = 300$–400 nm. No PS formation on *p*-Si	Noguchi and Suemune (1993)
n (0.4–0.7)	Anhydrous and hydrous HF	W lamp (undispersed)	~2.0	PS is formed only on the metal-backed Si substrates. PS layer thickness: ~300–500 nm	Zhang et al. (1993)
n (5–8)	32% HF	Ar laser, Xe lamp (465–780 nm)	~1.7–1.9	PL peak energy depends on photoetching wavelength	Cheah and Choy (1994)
n (2), *p* (2)	40% HF	HeNe laser	~1.7–2.0	PS is easily formed on the back surface of the sample PS is formed on both *n*-Si and *p*-Si. PL peak energy depends on excitation (PL) wavelength	Andersen et al. (1995)
n	$2HF{:}1HNO_3{:}4H_2O$	Gas, dye, and solid-state lasers	~1.9–2.2	The shorter the photoetching wavelength, the higher the PL peak energy. The higher the photoetching laser power, the higher the PL peak energy	Jones et al. (1996)
n (4.5–6.4)	48% HF	Gas and solid-state lasers	~1.8–2.3	The shorter the photoetching wavelength, the higher the PL peak energy	Kolasinski et al. (2000)
n (35–45)	$6HF{:}1H_2O_2$	HeNe laser	~1.8–1.95	Blue luminescence (420 nm) after dipping in $1C_2H_5OH{:}1H_2O$ for 148 h	Yamamoto and Takai (2000)
n (0.22–0.38, 35–45)	100HF: (17–250) H_2O_2	HeNe laser	~1.9–2.0	PL intensity is shown to strongly depend on etching solution composition and time	Yamamoto and Takai (2001)
n (10)	40% HF	Nd:YAG laser (1064 nm), Ar laser (514 nm)	~1.9–2.0	A two-peak (1.91 and 2.02 eV) structure in the PL spectrum (Ar laser). A single PL peak at ~2.0 eV (Nd:YAG laser)	Mavi et al. (2001)
n (4.5–10.4)	HF:(K^+, Cs^+, or Rb^+), etc.	HeNe laser	~2.0–2.1	Hexafluorosilicate-coated PS exhibiting blue-shifted PL emission	Koker et al. (2002)

(*continued*)

Table 1 (continued)

Type (Ω cm)	Solution	Light source	PL peak energy (eV)	Comments	References
n (1–5)	$1HF:1H_2O_2$	HeNe laser	~1.7–1.9	PL peak energy is dependent on excitation light wavelength	Marotti et al. (2003)
n (3–5)	40% HF	Ar laser	1.91, 2.05	Nanoparticle size is dependent on laser power density and irradiation time	Mavi et al. (2006)
n (4–6)	49% HF	Synchrotron X-ray beam	~1.94	Strong white X-ray beam illumination electropolishes, while a weak monochromatic X-ray beam makes the Si surface porous	Cho et al. (2006)
n (1–3)	$HF:KIO_3:H_2O$	Xe lamp (<600 nm)	~1.9–2.0	PS layer thickness: ≤75 nm	Xu and Adachi (2006)
n (1–3)	$HF:I_2:H_2O$	Xe lamp (<600 nm)	~1.0–2.0	PL intensity is about 380 times stronger than that synthesized in pure HF solution	Adachi and Kubota (2007)
n (1–3)	$HF:I_2:H_2O$	Xe lamp (<600 nm)	~2.0	Studying a correlation between PL properties and other spectroscopic characteristics (spectroscopic ellipsometry, photovoltage, photoconductivity, etc.)	Adachi and Oi (2007)
n (1–3)	$HF:FeCl_3:H_2O$	Xe lamp (<600 nm)	~1.8–2.0	PS layer thickness: ≤650 nm	Xu and Adachi (2007)
n (1–3)	$HF:H_2O_2:H_2O$	Xe lamp (<600 nm)	~1.8–2.0	Demonstrates the effectiveness of SPM clearing for stable PS formation	Tomioka et al. (2007)
n (1–3)	$HF:KIO_3:H_2O$	Laser diode (532 nm)	~1.9–2.0	A strong light-emitting PS layer can be formed in the limited KIO_3 concentration	Xu and Adachi (2008)
n (0.75)	40% HF	Laser diode (635 nm)	~1.8–2.0	Laser power dependence of PS layer morphology	Ramizy et al. (2011)
n (10–20)	$8HF:1H_2O_2$	Xe lamp (<600 nm)	~1.0–2.0	A new approach to forming PS layer using a closed-circuit anodic system under light illumination without an external voltage	Matsui and Adachi (2012)

Table 2 Photoetching for porous silicon formation in alkaline electrolytes and aqueous alkali salt solutions

Type (Ω cm)	Solution	Light source	PL peak energy (eV)	Comments	References
	25% TMAH	Nd:YAG laser (1064 nm)	No PL study	Macroporous structure	Zheng et al. (2005)
n (13–20)	1 M KF	HeNe laser	~3.3 eV	An HF-free technique	Tomioka and Adachi (2005)
n (13–20)	Spa water (pH ~ 10.5)	HeNe laser	~2.0	An HF-free technique	Adachi and Tomioka (2005)
n (10–20)	1 M NaF 1 M KF	HeNe laser	~2.7–2.8 eV and ~3.3 eV	An HF-free technique	Adachi et al. (2007)

TMAH tetramethyl ammonium hydroxide

Adachi 2006, 2007, 2008; Adachi and Kubota 2007; Adachi and Oi 2007; Tomioka et al. 2007; Adachi et al. 2007; Ramizy et al. 2011; Matsui and Adachi 2012).

To the best of our knowledge, there has not been reported any good plan-view high-resolution scanning electron microscopy images of the photosynthesized PS layers showing the morphology of their typical structures. In Xu and Adachi (2007), the atomic force microscopy images were reported to show many irregularly shaped hillocks and voids distributed randomly over the entire PS surface. The observed root-mean-squares roughnesses were a few nanometers.

Lateral patterning of PS layers has been performed using photoassisted electrochemical etching rather than pure photoetching (Baranauskas et al. 1995; Diesinger et al. 2003). Lateral modification of the porosity has also been obtained by photochemical dissolution of the anodic PS layers under illumination with a beam made of interference fringes (Ferrand et al. 2001).

A metal-insulator-semiconductor-type electroluminescent (EL) device has been fabricated from PS layers synthesized by photoetching in an HF/I_2 solution (Adachi and Kubota 2008). An insulating layer was formed on the PS layer by chemical oxidation in an acidic solution. Spectral output of the EL device was in the red-yellow region peaking at 2 eV.

Photoetching of Silicon Powders

The enhanced etching of bulk silicon in hydrofluoric acid via continuous photoexcitation has been known for a long time and has been used to pattern wafers (Lim et al. 1992). Recently, the technique has received some development for nanostructuring of inexpensive silicon powders (Matsumoto et al. 2014, Lee et al. 2016) in addition to silicon wafers. Although TEM and XRD data demonstrated the presence of silicon nanoparticles (Matsumoto et al. 2014, Lee et al. 2016), it would be interesting to explore with gas adsorption analysis (see handbook chapter

► "Gas Adsorption Analysis of Porous Silicon") whether significant mesoporosity can be engineered in such processed powders.

Conclusions

Photoetching enables the formation of a visible light-emitting PS layer on *n*-type Si wafers. The use of an incoherent light source and the addition of an oxidizing agent in the HF solution also facilitate the formation of a thicker homogeneous PS layer with good reproducibility. The thickness of the porous layer is still usually less than 1 μm. The PL and EL peak energies were observed to be in the range 1.7–2.3 eV. The photoetching technique can be applied to Si wafers with embedded circuitry, SOI wafers, and silicon powders.

References

Adachi S, Kubota T (2007) Light-emitting porous silicon synthesized by photoetching in aqueous HF/I_2 solution. Electrochem Solid St 10:H39–H42

Adachi S, Kubota T (2008) Electroluminescence from porous silicon formed by photoetching in an HF/I_2 solution. J Porous Mater 15:427–431

Adachi S, Oi M (2007) Spectroscopic investigation of light-emitting porous silicon photoetched in aqueous HF/I_2 solution. J Appl Phys 102:063506-1–063506-9

Adachi S, Tomioka K (2005) Visible light emission from porous silicon prepared by photoetching in alkaline solution. Electrochem Solid St 8:G251–G253

Adachi S, Miyazaki T, Inoue K, Sodezawa S (2007) Light emission from porous silicon photoetched in aqueous alkali salt solutions. Jpn J Appl Phys 46:4028–4034

Andersen OK, Frello T, Veje E (1995) Photoinduced synthesis of porous silicon without anodization. J Appl Phys 78:6189–6192

Baranauskas V, Thim GP, Peled A (1995) Laser-induced formation of porous silicon. Appl Surf Sci 86:398–404

Canham LT (1990) Silicon quantum wire array fabricated by electrochemical and chemical dissolution of wafers. Appl Phys Lett 57:103561–103563

Cheah KW, Choy CH (1994) Wavelength dependence in photosynthesis of porous silicon dot. Solid State Commun 91:795–797

Cho IH, Kim DH, Noh DY (2006) X-ray photochemical wet etching of n-Si (100) in hydrofluoric solution. Appl Phys Lett 89:054104-1–054104-3

Diesinger H, Bsiesy A, Hérino R (2003) Nano-structuring of silicon and porous silicon by photoetching using near field optics. Phys Status Solidi A 197:561–565

Ferrand P, Romestain R, Vial JC (2001) Photonic band-gap properties of a porous silicon periodic planar waveguide. Phys Rev B 63:115106-1–115106-4

Jones LA, Yükseker Ö, Thomas DF (1996) Dependence of photochemically etched porous silicon formation on photoetching wavelength and power. J Vac Sci Technol A 14:1505–1510

Kobayashi Y, Adachi S (2010) Structural and optical properties of Si nanowires synthesized by galvanic cell reaction. Jpn J Appl Phys 49:075002-1–075002-7

Koker L, Wellner A, Sherratt PAJ, Neuendorf R, Kolasinski KW (2002) Laser-assisted formation of porous silicon in diverse fluoride solutions: hexafluorosilicate deposition. J Phys Chem B 106: 4424–4431

Kolasinski KW, Barnard JC, Ganguly S, Koker L, Wellner A, Aindow M, Palmer RE, Field CN, Hamley PA, Poliakoff M (2000) On the role of the pore filling medium in photoluminescence from photochemically etched porous silicon. J Appl Phys 88:2472–2479

Lee YI, Kim BS, Joo S, Kim WB (2016) Low cost fabrication of blue luminescent silicon quantum dots using photoinduced chemical etching. Nanosci Nanotechnol Lett 8:86–89

Lim P, Brock JR, Trachtenberg I (1992) Laser-induced etching of silicon in hydrofluoric acid. Appl Phys Lett 60:486–488

Marotti RE, Quagliata E, Dalchiele EA (2003) Photoluminescence from photochemically etched silicon. Sol Energy Mater Sol Cells 76:263–279

Matsui Y, Adachi S (2012) Optical properties of porous silicon layers formed by electroless photovoltaic etching. ECS J Solid State Sci Technol 1:R80–R85

Matsumoto T, Maeda M, Furukawa J, Kim WB, Kobayashi H (2014) Si nanoparticles fabricated from Si swarf by photochemical etching method. J Nanopart Res 16:2240-1–2240-7

Mavi HS, Rasheed BG, Soni RK, Abbi SC, Jain KP (2001) Photoluminescence and Raman study of porous silicon synthesized by visible and infrared laser etching. Thin Solid Films 397:125–132

Mavi HS, Prusty S, Kumar M, Kumar R, Shukla AK, Rath S (2006) Formation of Si and Ge quantum structures by laser-induced etching. Phys Status Solidi A 203:2444–2450

Noguchi N, Suemune I (1993) Luminescent porous silicon synthesized by visible light irradiation. Appl Phys Lett 62:1429–1431

Peter LM, Blackwood DJ, Pons S (1989) In situ characterization of the illuminated silicon-electrolyte interface by Fourier-transform infrared spectroscopy. Phys Rev Lett 62:308–311

Ramizy A, Hassan Z, Omar K (2011) Laser-induced etching parameters impact on optical properties of the silicon nanostructures. Sci China Technol Sci 54:58–62

Saxena SK, Kumar V, Rai HM, Sahu G, Late R, Saxena K, Shukla AK, Sagdeo PR, Kumar R (2015) Study of porous silicon prepared using metal-induced etching (MIE): a comparison with laser-induced etching (LIE). Silicon. doi: 10.1007/S12633-014-9242-y

Tomioka K, Adachi S (2005) Strong and stable ultraviolet emission from porous silicon prepared by photoetching in aqueous KF solution. Appl Phys Lett 87:251920-1–251920-3

Tomioka S, Miyazaki T, Adachi S (2007) Porous silicon formation by photoetching in HF/H_2O_2 solution using incoherent light source. Jpn J Appl Phys 46:5021–5024

Xu YK, Adachi S (2006) Light-emitting porous silicon formed by photoetching in aqueous HF/KIO_3 solution. J Phys D Appl Phys 39:4572–4577

Xu YK, Adachi S (2007) Properties of light-emitting porous silicon photoetched in aqueous HF/$FeCl_3$ solution. J Appl Phys 101:103509-1–103509-5

Xu YK, Adachi S (2008) Properties of light-emitting porous silicon formed by stain etching in HF/KIO_3 solution under light illumination. J Appl Phys 103:103512-1–103512-6

Yamamoto N, Takai H (2000) Visible luminescence from photo-chemically etched silicon. Thin Solid Films 359:184–187

Yamamoto N, Takai H (2001) Formation mechanism of silicon based luminescence material using a photo chemical etching method. Thin Solid Films 388:138–142

Zhang Z, Lerner MM, Alekel T III, Keszler DA (1993) Formation of a photoluminescent surface on n-Si by irradiation without an externally applied potential. J Electrochem Soc 140:L97–L98

Zheng HY, Chai JC, Lam YC, Zhu H (2005) Formation of porous structures on Si surface by laser-assisted etching. Surf Rev Lett 12:351–354